Reservoir Modeling And Production History Matching In A Triassic Naturally Fractured Carbonate Reservoir In Sichuan, China

Minh Vo*, **San Su**, and **Jianjiang Lv**, Chevron Unocal East China Sea Ltd, Chengdu, China;
Chaohong Xiao, Southwest Oil and Gas Company, CNPC, Chengdu, China

Abstract

Fractures are observed on the image log data in many Triassic carbonate gas fields in the block located in Sichuan Basin, China, and clearly matched at the equivalent analogy outcrops. The pressure transient analysis test (PTA) after the field's First Gas clearly implies a dual porosity dual permeability system. Sustained high gas rate from all producing wells and the communication between two well pads in distant indicate the significant role fractures play in well deliverability.

To support flow simulation, Discrete Fracture Networks (DFN) modelling was conducted with various static data as inputs. Multivariate Analysis (MVA) was carried out to ensure a quality correlation between reservoir and fracture properties which is the key for fracture modelling. The k_{max}/k_{min} ratio of the resulting elliptical fracture permeability tensors were scaled to an uncertainty range defined by integrating the core and FMI interpretation, equivalent outcrop study, and analogy data. The tensors throughout the model were then calibrated to the fracture component of isotropic permeability derived from well test.

Prior to the simulation, the single well Inflow Performance Relationships (IPR) was calibrated to actual flow test results by adjustment in the simulation model. The production forecast shows that the reservoir depletion profile from the simulation model overlaps well with P/z versus three-year cumulative production based on PTA results, and the single well production from the simulation model matches actual data, indicating a reliable static reservoir model and dynamic simulation process.

In brief, this presentation is to share the fit-for-purpose approach of reservoir modelling and history matching which has greatly helped better understand the dynamic performance of the reservoir, and therefore to guide optimal field development. The success can be tailored to other fields of similar kind.

Introduction

This greenfield sour gas project is developed in Sichuan, China. The full field development schematics is shown in **Figure 1.**

DOI: 10.14800/IOGR.1155
Received February 28, 2020; revised May 4, 2019; accepted May 13, 2020.
*Corresponding author: minh.vo@chevron.com

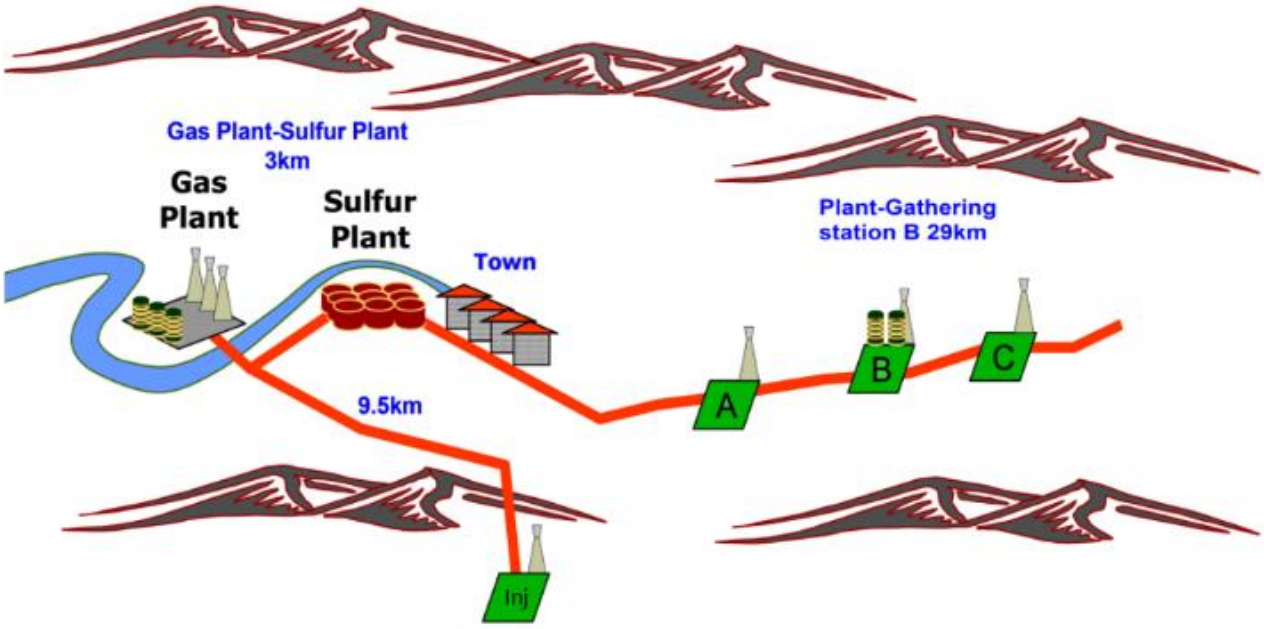

Figure 1—Sour gas development project.

The project involves development of gas resources in Triassic carbonate reservoirs. The field of interest is made up of bedded dolomite and limestone lithofacies of Early Triassic age. The depositional environment is carbonate platform margin and ramped with oolitic shoals. Gas is trapped in thrust-related anticlinal structures and seals comprise tight limestones and anhydrites. The structure is normally large. The reservoir fluid is dry gas, with H_2S and CO_2.

Fractures in Reservoir and Their Impact

Fractures are a universal element in sedimentary rock layers (Nelson 2001), and they are more common in carbonate rocks with higher brittleness than in sandstones (Crain 2017; Kuchuk et al. 2015).

Natural fractures in carbonate reservoir can help create secondary porosity and promote communication between reservoir compartments. However, fractures may sometimes short-cut fluid flow within a reservoir, causing early water production (Bratton et al. 2006). Therefore, it is very important to characterize and model fractures to determine their effect in our reservoir performance. With the understanding of the regularity of fractures distribution, wells can be planned effectively and efficiently to maximize production. In development drilling program (if there are any), appreciation of fractures' impact on reservoir connectivity can prevent from drilling redundant wells to manage cost and to maximize the value of the field development. In fact, naturally fractured reservoirs are very complicated and difficult to evaluate due to: 1) lack of in-depth quantitative approaches for the description and characterization of highly anisotropic reservoirs; 2) failure to recognize fractures and their distribution; 3) over-simplistic approaches in the description of fractures distributions and morphologies; and 4) data limitations only allowing stochastic rather than deterministic fluid flow simulation (Nelson 2001; Bourbiaux et al. 2005).

Within the area of interest in this study, there are 5 Triassic dolomite gas fields. Both static information from cores, logs and equivalent outcrops, and dynamic information from well-test data since field production demonstrate the presence of natural fracture development in the carbonate reservoirs. In recognizing the challenges and significance of natural fractures, this paper is trying to fully utilize all sorts of static and dynamic fracture data to characterize and model fractures in the reservoirs, which therefore enables us to evaluate the impact of fractures on production and guide optimal future development.

Fracture Characterization

Various approaches can be carried out to characterize natural fractures in the reservoirs to assist fracture modelling, including equivalent outcrop study, FMI interpretation, and well-test analysis. Application of 3D seismic attributes, unfortunately not applicable in this study due to data quality and resolution, is also proved to be an effective way to characterize fracture network (Angerer et al. 2011).

Equivalent Outcrop Analog. As showing in **Figure 2**, vertical fractures can be observed in the equivalent outcrop of reservoir rocks. As the outcrops are in the cliffs near top of the mountain, fracture parameters such as density, aperture, length, dip and azimuth data could not be obtained due to the inaccessibility. Given reservoir model cell size of 200 m × 200 m × 7 m in this study, fractures in the photo would penetrate multiple vertical cells.

FMI Interpretation of Fracture Density & Orientation. Interpretation of images logs has suggested that open fractures should play an important role in the reservoir flow. However, the absence of important ancillary flow data (such as production logging test) hinders determination of fracture system flow effectiveness. In fact, it is only through interrogation of a variety of different data types that the characteristics of fractured reservoir are revealed (Narr et al. 2006).

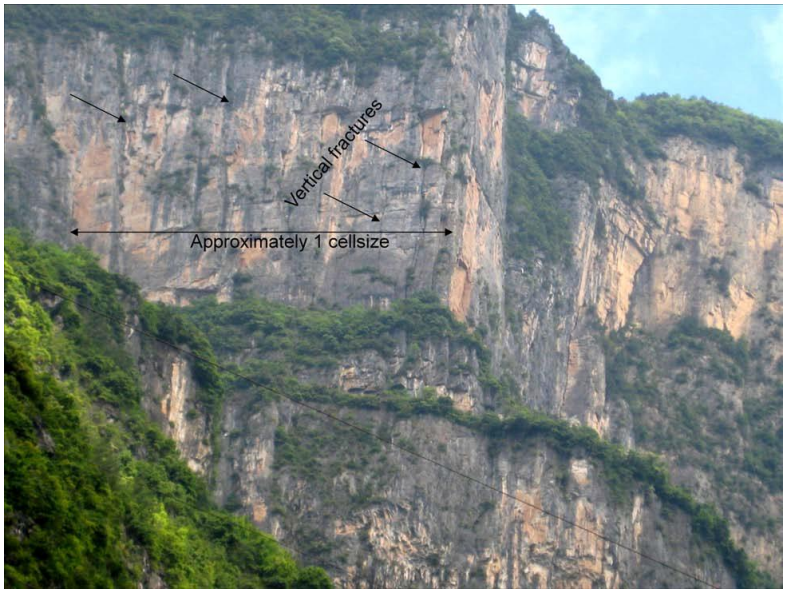

Figure 2—Persuasive large-scale vertical fractures on equivalent outcrops.

Figure 3 shows the fracture interpretation from FMI image logs. The same fracture interpreted from image log is also identified in the equivalent core.

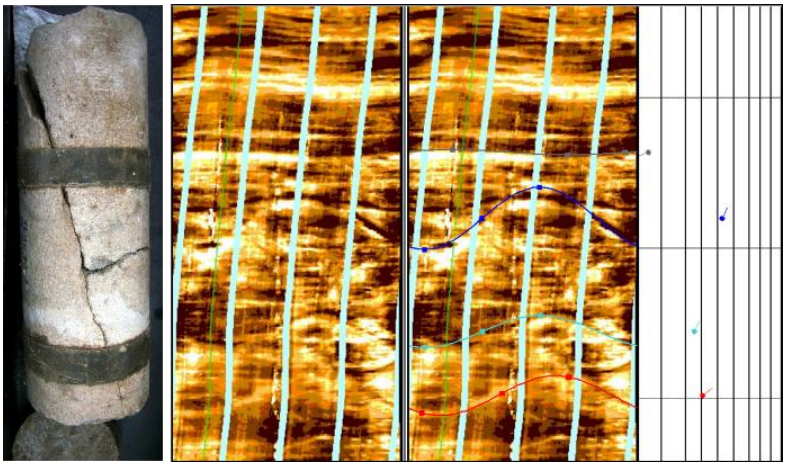

Figure 3—Fracture interpreted from FMI in comparing with the fractures observed on core of well A.

Figure 4 shows the fracture parameters interpreted from FMI log of Well A in Field A. Fracture density is calculated using the methodology as described by Wayne Narr (Narr 1996). Fracture orientations are plotted in rose diagram for easy visualization. The fractures interpreted from Well A image log are parallel to the strike of the anticline (**Figure 5**), which is the dominant fracture orientation in Field A as well as the other offset fields. Another well in Field A has a majority fracture orientation perpendicular to the strike of the anticline, and it represents the secondary fracture orientation.

The conceptual fracture model can be constructed based on fracture parameters interpretation, rock competency evaluation, tectonic stress analysis and analogous structures. In a typical asymmetric anticline, there are three types of fractures, including hinge-parallel fractures, hinge-perpendicular fractures and oblique fractures (Figure 5) (Price 1966; Stearns and Friedman 1972; Aguilera 1980; Price and Cosgrove 1990; Awdal et al. 2016; Galuppoc et al. 2016). The hypothesis is that hinge-perpendicular fractures are pre-folding whereas hinge-parallel and oblique fractures are fold-related or post-folding fractures.

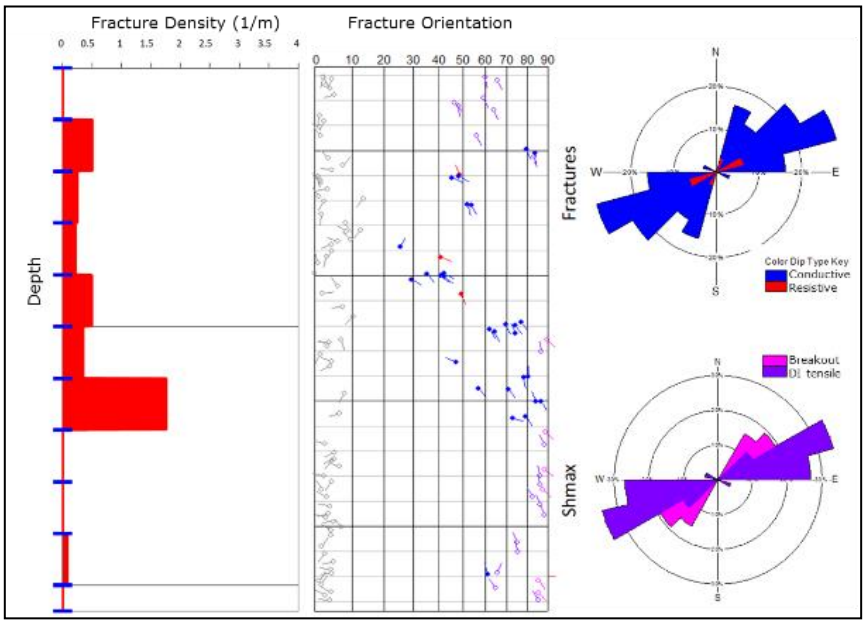

Figure 4—Fracture density and orientation interpreted from FMI image log from Well A.

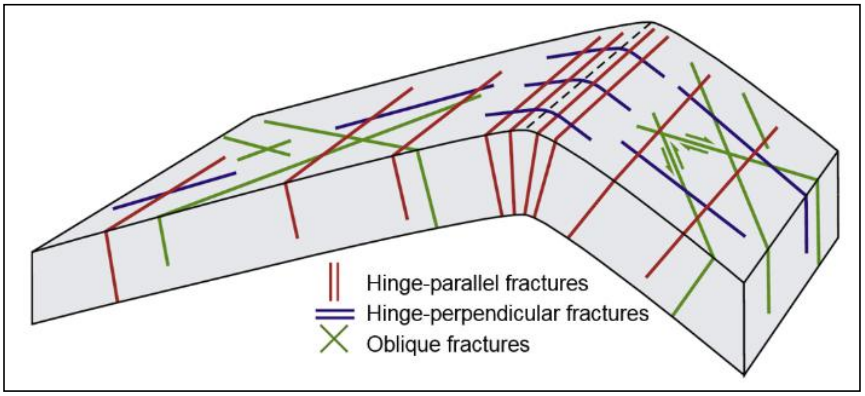

Figure 5—Observed fracture sets shown in Price's classification of fracture sets typical for asymmetric anticlines.

The Field A in this study is characterized as an asymmetric anticline trending NE-SW by 3D seismic data and well data. Based on the limited FMI data (2 wells in the field) and FMI data from the offset fields, the conceptual fracture sketch for Field A is generated as shown in **Figure 6**. The dominant fracture orientation is parallel to the strike of the anticline, with secondary fracture orientation being perpendicular or oblique to the strike.

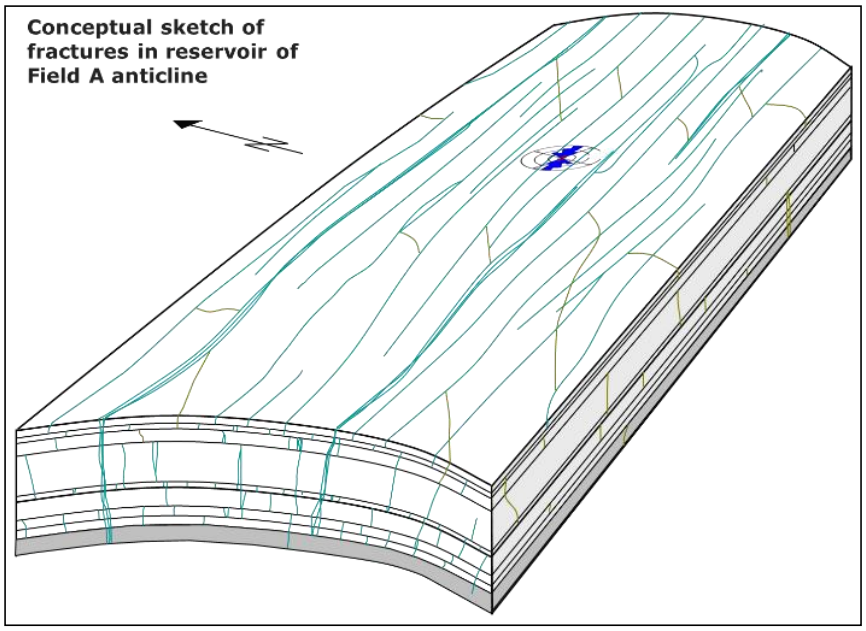

Figure 6—Field A conceptual fracture development and distribution (courtesy Wayne Narr).

Fracture Characteristics from Well-Test Data. Diagnostic plot can be constructed to identify various flow regimes and reservoir heterogeneities as these affect the pressure response during well-test (Satter and Iqbal 2015). Naturally fractured reservoirs have two distinct porosities, one in the matrix and one in the irregular fractures (Fekete 2017), and they can be represented by equivalent homogenous dual porosity systems (Lee and Wattenbarger 1996).

In a dual porosity system, flow from both the fractures and matrix are assumed. A characteristic "dip" is observed in the derivative plot (**Figure 7**) beyond the wellbore storage effects. Flow from a highly conductive fracture system leads to less pressure change over time, causing the apparent dip, which is often referred as "dual porosity dip" (Satter and Iqbal 2015), and is defined by two parameters including ω and λ. ω is the storability ratio and is essentially the fraction of hydrocarbon stored in the fracture system. It determines the depth of the dip, with smaller ω corresponding to deeper dip. λ is the inter-porosity flow coefficient that characterizes the ability of gas flowing from matrix to fractures.

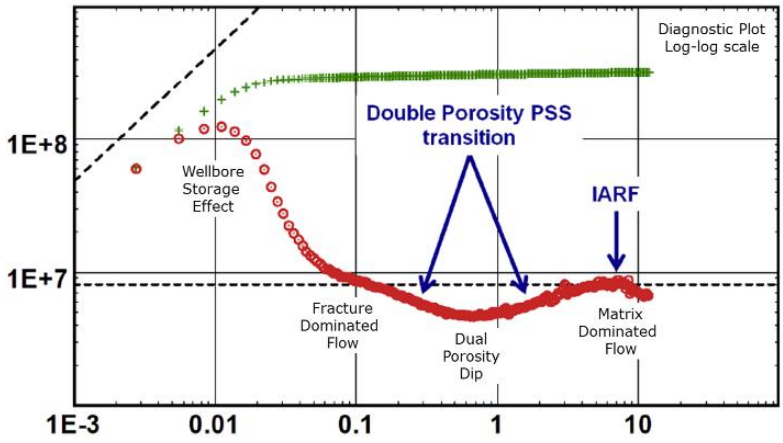

Figure 7—Signature of a dual porosity reservoir on a diagnostic plot.

It also determines the time of start of transition (from fracture dominated flow to matrix dominate flow) and controls the speed at which the matrix will react, with smaller λ corresponding to later dip. A reservoir with a big λ has relatively high matrix permeability, so it will start to give up its fluid almost as soon as the fracture system starts to produce, and vice versa (Kappa 2017).

Prior to the field production, the well-test data is limited as the duration was not long enough to represent the full reservoir behavior. Quality well-test data after Field A on production was recorded through permanent downhole pressure gauge during the pressure build-up test when the well was shut in. The interpretation of the well-test data clearly indicates a dual porosity system (**Figure 8**) (Satter and Iqbal 2015; Kappa 2017).

The shallower "dip" on the PTA analysis plot implies a relatively large ω, and that the pressure support from the matrix during the transition is relatively less substantial. Such feature indicates that the fractures account for a large portion of pore volume. The λ in this case is about 10^{-7}, a moderate value which might show that the matrix is neither too tight nor too porous, and moderate pressure drawdown will have to be established in the fractures system before the matrix will appreciably give up any fluid (Kappa 2017), and the transition starts neither too early nor too late.

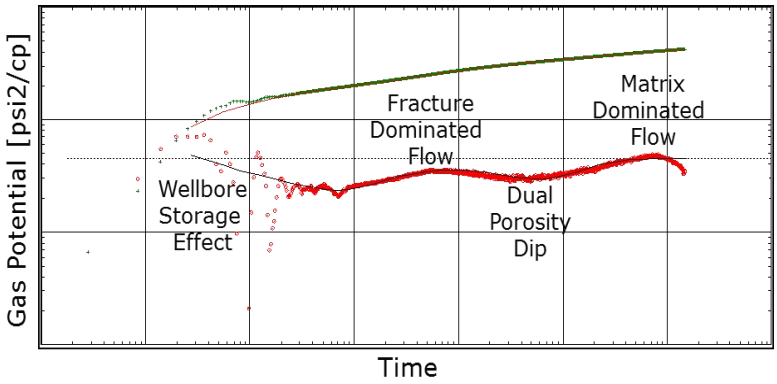

Figure 8—Well B dual porosity model as interpreted from PTA.

The dynamic characteristics of permeability of the fractures and matrix as revealed by well-test data should be integrated with static characterization to construct the fracture model.

Fracture Modeling Workflow

With relatively good understanding of the fracture characteristics in the reservoirs, static fracture modeling can be carried over to further assist flow simulation.

The fracture modeling workflow consists two parts. The first part is to model the fractures using fit-for-purpose fracture modeling technique based on mainly on static reservoir information prior to field

production. The second part is to calibrate the above fracture model to dynamic reservoir parameters as derived from production performance and well-test.

The fracture modeling workflow suggested by SMEs is showing in **Figure 9**. Firstly, the fractures are interpreted from available image logs, the fracture density curves are calculated, and the fracture orientation and distribution regularity with regarding to the structure are understood.

Secondly, the correlations between calculated fracture density and reservoir properties which have been populated in the reservoir model is established. This step is usually very challenge due to limit fracture density data, and the correlation coefficient largely determines the quality of the resulting fracture model. With the establishment of such correlation, fracture density in each grid cell can be predicted from the reservoir property in the same cell. The potential reservoir properties that can be used to correlate with and predict fracture density include but not limit to facies, porosity, formation, seismic anomaly and geometric factor, etc.(Narr et al. 2004).

The next step is to develop reasonable uncertainty ranges for a series of fracture parameters including fracture density, azimuth, length, mean aperture, and through-going fracture length cutoff, aiming to capture a wide yet realistic range of simulation outcomes.

The final step is to create a discrete fracture model using fracture density which already populated in the whole grid model and the fracture parameters as defined above. The discrete fractures are then effectivized into permeability tensor. The output of the fracture modeling is the horizontal fracture permeability tensor in each grid cell. The tensor can be then combined with matrix permeability as the composite horizontal permeability.

The fracture parameters' sensitivity on gas production can be evaluated. The big hitters identified from the sensitivity study could be included in the dynamic experimental design to optimize the flow simulation while capturing all possible scenarios.

The modeled fracture permeabilities based on static data usually have a large uncertainty range, and they should be scaled and calibrated to dynamic permeability as derived from well test analysis.

Fracture Model Calibrated with Dynamic Data

The static fracture model constructed following the above steps has several limitations. Firstly, the input data availability and quality are usually limited and compromised. Secondly, the static fracture model normally has multi-million grid cells depending on the reservoir areal extension and thickness, while the popular flow simulator usually cannot handle model with so many grid cells efficiently, thus requiring an up-scaling process before the actual flow simulation. The up-scale process shall of course lose part of the reservoir information. The advances in technology such as next generation simulator which is deemed to handle a larger number of cells in a less time-consuming manner should help to eliminate the issues brought by up-scaling process. Therefore, it is of necessity to update the static fracture model with dynamic performance data after the field is on production for a reasonable amount of time. The authors herein introduce a fit-for-purpose adjustment technique to revise the model.

The permeability derived from well-test (k_{iso}) is a composite property of matrix and fracture permeability. The fracture permeability (k_{isof}) can be calculated by subtracting matrix permeability (k_{isom}) from well-test permeability k_{iso} (i.e. $k_{isof} = k_{iso} - k_{isom}$). The fracture model adjustment is indeed the calibration of fracture permeability only.

The adjustment of fracture permeability includes two steps.

- The first step is to scale the permeability tensor to the desired major-axis / minor-axis ratios (i.e. k_{maxf}/k_{minf} ratios). This step can be skipped if the static fracture model is considered as reasonable.
- The second step is to calibrate the static fracture permeability in the model to fracture permeability derived from well-test.

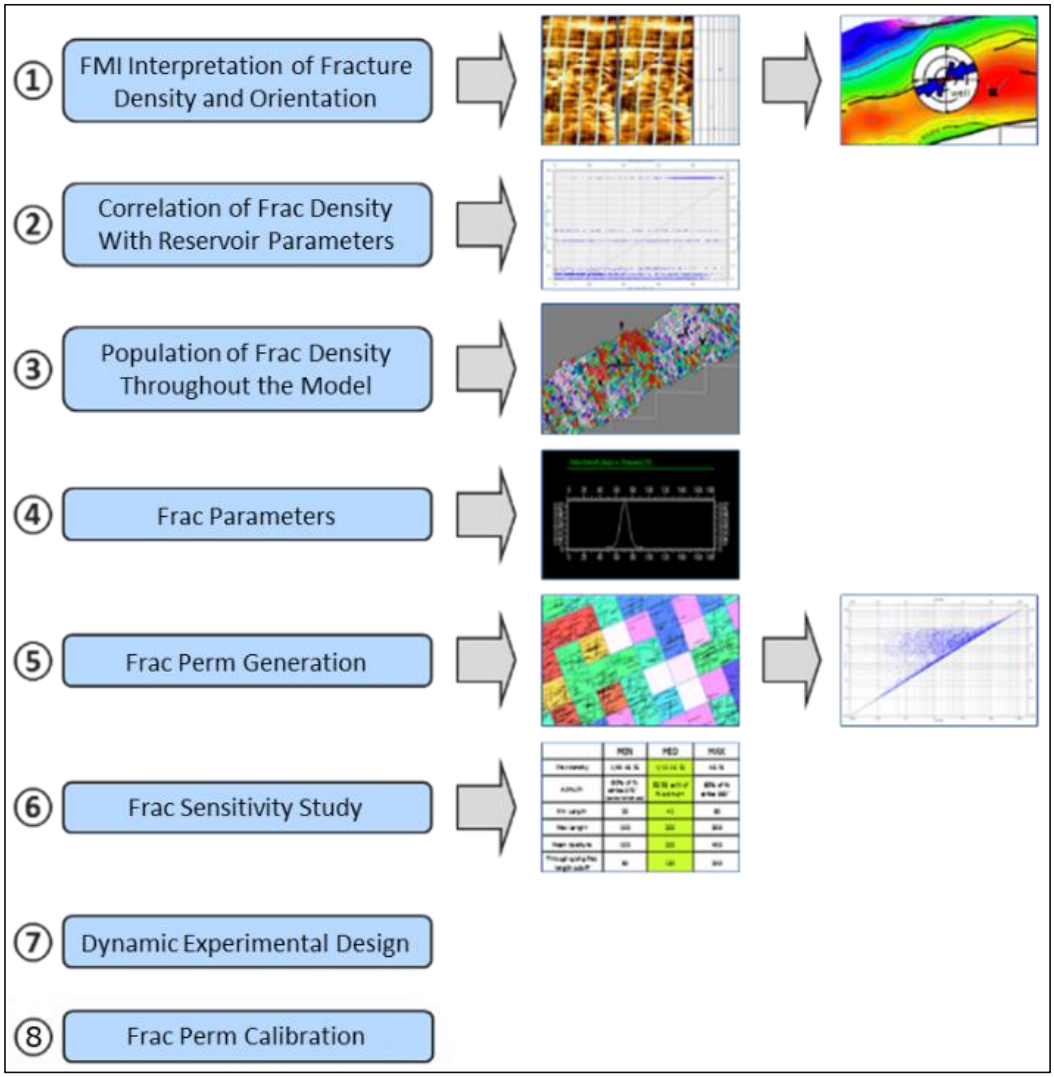

Figure 9—Fracture Modelling Workflow (courtesy Eric A. Flodin and Jerome Glass).

Scaling Permeability Tensor. Due to the availability and quality of input data for fracture modelling, the ratio between k_{maxf} and k_{minf} of the permeability tensor in the fracture model may not be reasonable. Therefore, it is necessary to scale the ratio and confine it to an uncertainty range of Min-Mid-Max, which is defined by fracture SMEs based on the understanding of reservoirs of similar kinds, and of course, local and regional benchmark data.

To achieve the desired uncertainty range, firstly the k_{maxf}/k_{minf} ratio in each grid cell in area of interest (AOI) needs to be scaled to "Mid" ratio while keeping the average isotropic fracture permeability in AOI unchanged. The next step is to scale the ratios to "Min" and "Max" in the regions where the k_{maxf}/k_{minf} ratio is less than "Min" and greater than "Max" respectively and keep the average isotropic fracture permeability in the regions unchanged as well (**Figure 10**).

The scaling process ensures the k_{maxf}/k_{minf} ratio in the AOI falling in the desired uncertainty ratio of Min-Mid-Max, while the average fracture permeability is unchanged.

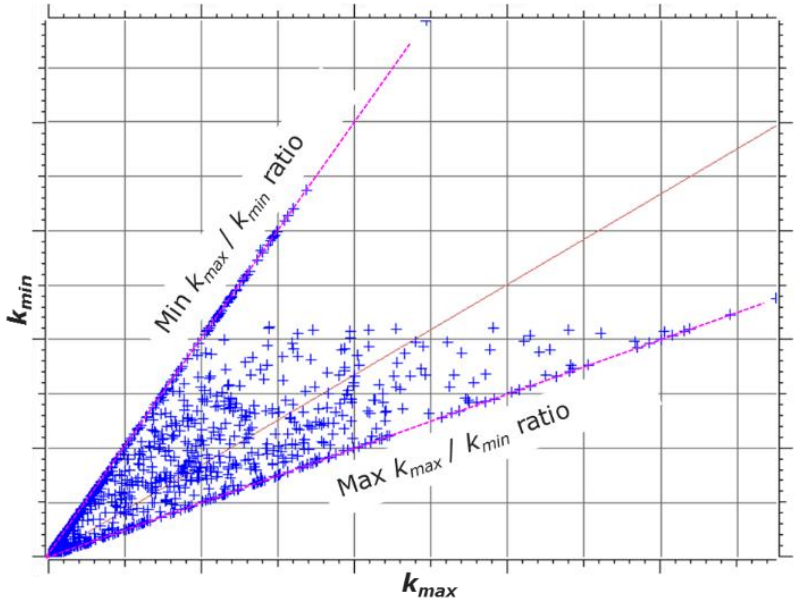

Figure 10—Scaling of k_{max}/k_{min} Ratio in Fracture Model.

Static Permeability to Dynamic Permeability. The static fracture permeability tensors after scaling need to be calibrated to fracture component of permeability derived from well-test (k_{isof}).

As shown in **Figure 11**, k_{iso} can be considered as an equivalent isotropic permeability of the k_{max} and k_{min} on permeability tensor. k_{iso} is the geometric mean of k_{maxf} and k_{minf} as shown

$$k_{isof}{}^2 = k_{maxf\_c} \times k_{minf\_c} \quad (1)$$

Similarly, the well-test derived fracture permeability k_{isof} should be equal to geometric mean of calibrated k_{maxf_c} and k_{minf_c}, as shown

$$k_{isof}{}^2 = k_{maxf\_c} \times k_{minf_c}, \quad (2)$$

To keep the ratio between major axis and minor axis of the fracture permeability tensors unchanged during the calibration process, we have

$$\frac{k_{maxf\_c}}{k_{minf\_c}} = \frac{k_{maxf}}{k_{minf}} \quad (3)$$

Solve **Eqs. 2** and **3**, the k_{maxf_c} and k_{minf_c} as final anisotropic fracture permeability can be calculated as

$$k_{maxf\_c} = \sqrt{k_{isof}{}^2 \times \frac{k_{maxf}}{k_{minf}}}, \quad (4)$$

$$k_{minf\_c} = \sqrt{k_{isof}{}^2 \times \frac{k_{minf}}{k_{maxf}}} \quad (5)$$

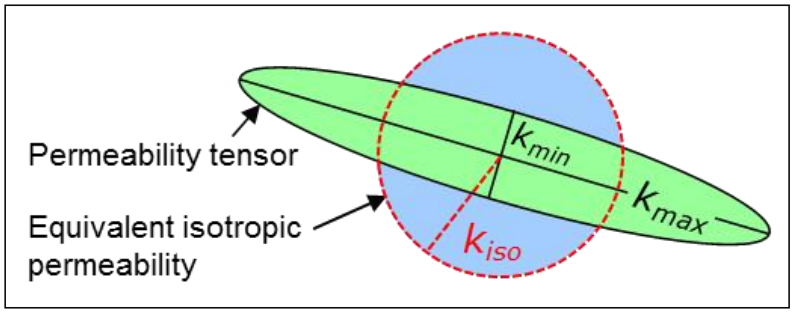

Figure 11—Permeability Tensor and the Equivalent Isotropic Permeability (Courtesy Wayne Narr).

After the above scaling and calibrating process, the fracture permeability tensor in each grid cell of AOI should have a reasonable k_{maxf}/k_{minf} ratio and the average fracture permeability in AOI should match the fracture permeability derived from well-test.

The adjusted fracture permeability is then added back to matrix permeability in corresponding grid cells as the final composite permeability for flow simulation.

IPR and VLP, Basics for Well Performance Calculation

Well-performance analysis, or 'Nodal Analysis', dictates that any single point (i.e. the bottom hole) must observe mass balance and can only have one pressure associated with it (Lyons and Plisga 2004). It is the normal practice that every petroleum engineer will do to understand the well potential and any improvement needed. A simplified model of Nodal Analysis is illustrated as a node in **Figure 12**.

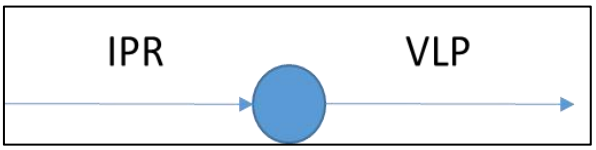

Figure 12—Nodal Analysis for Well Performance.

To make it simple, everything at upstream of the solution node will be treated as the 'IPR' and everything at downstream of the node will be part of the 'VLP'.

The IPR & VLP calculation allows to determine the production of a well for a set of conditions by combining the VLP and IPR curves in one plot. This means that the rate at which the VLP and IPR curves across (**Figure 13**) is the rate which the well will produce under these conditions such as wellhead pressure, water gas ratio, vertical lift correlation, solution, and wellbore structure.

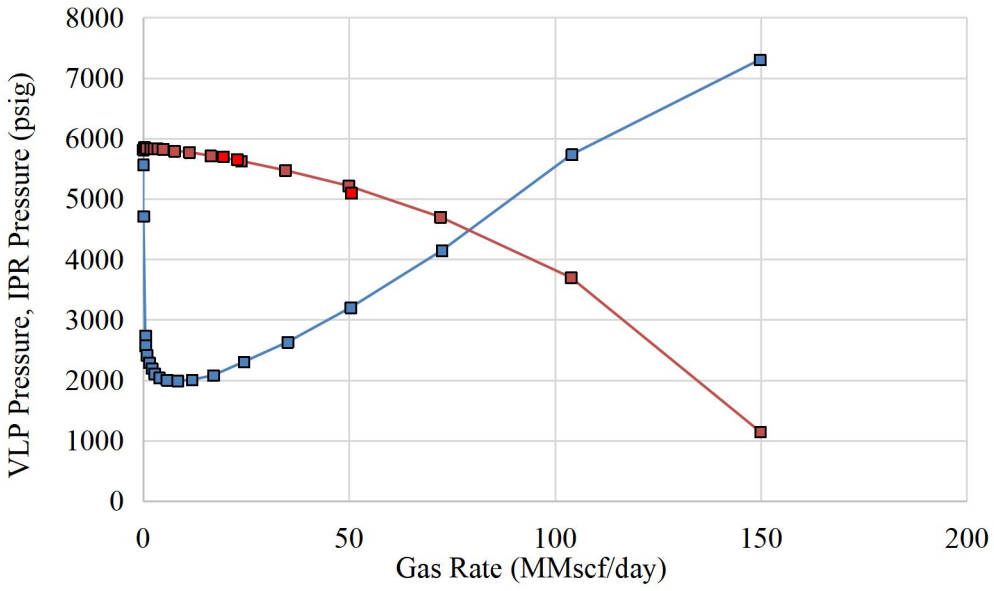

Figure 13—IPR & VLP Calculation Concept.

Best Fit Inflow Performance Relation (IPR)

The workflow can be illustrated in **Figure 14**. The first step is to figure out the best fit correlation from a built-in pool to convert WHP to BHP. Starting with the well that has both surface and downhole pressure gauges installed, the appropriate correlations are loaded to convert the surface pressure data to downhole pressure data, then the conversion results are compared with the actual PDHG data. Once the most

appropriate correlation is selected, two adjusting parameters can be applied to further calibrate it to match the exact data. One parameter is used to control the gravity (related to PVT) and the other is to control the friction loss (related to tubing roughness).

All the flow rates are thus determined from the actual well test performance as shown in **Figure 15**.

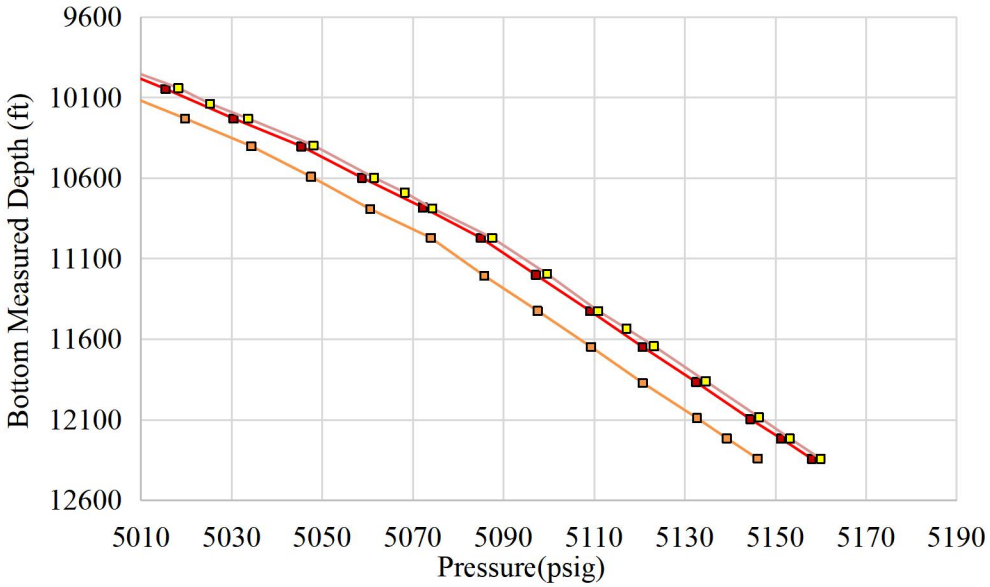

Figure 14—Using PDHG data for Best Fit Correlation.

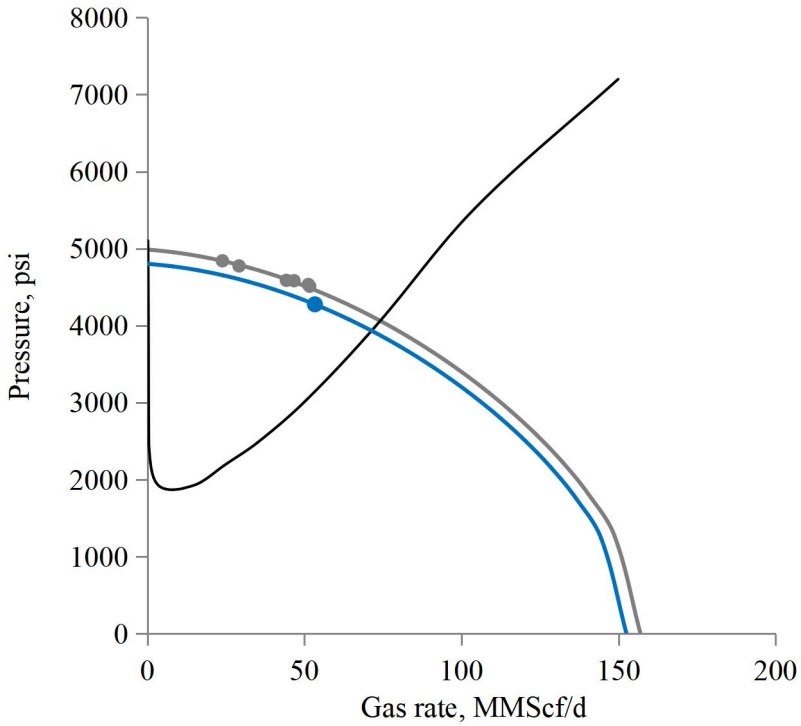

Figure 15—Well Performance from History Match.

This calibration workflow is applied to the other wells of similar structures but without PDHG, and all conversion results are with the good quality.

Best Fit Fractured Reservoir Performance

In addition to adjust the k_{maxf} /k_{minf} ratio to a reasonable Min-Mid-Max range (Mid case model) as illustrated above, the ratios in the AOI are also re-scaled to generate the Min and Max case models to test the sensitivity of permeability tensor (i.e. k_{maxf}/k_{minf} ratio).

In the Min case model, the k_{maxf}/k_{minf} ratio in all grid cell are scaled to the early-defined Min value, and similarly, the k_{maxf}/k_{minf} ratio in all grid cell are scaled to the early-defined Max value to generate the Max case model.

Flow simulation were then run on the Min, Mid and Max case models to quantify the impact of fracture permeability tensors. **Figure 16** displays the production profiles generated from the Min, Mid, and Max case models. The sensitivity analysis results as shown in **Table 1** conclude that the k_{maxf} /k_{minf} ratio uncertainty in Field A does not have a significant impact on either plateau length or pulse test response.

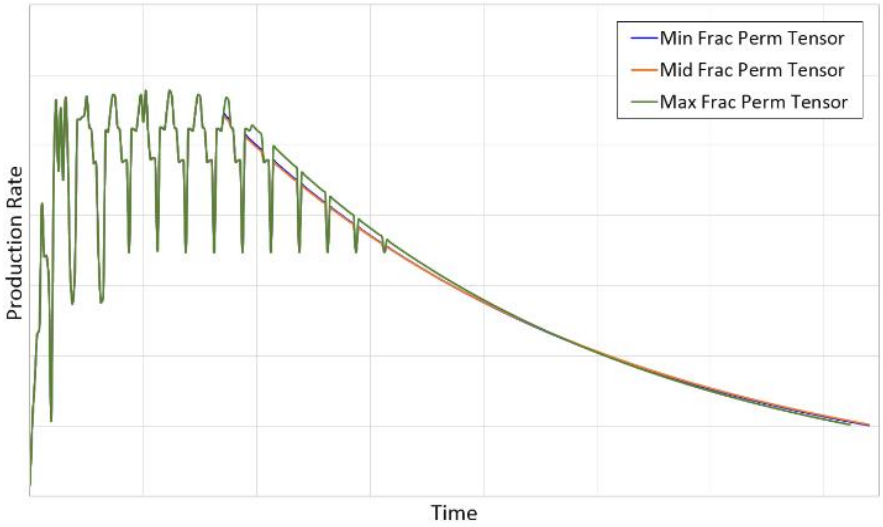

Figure 16—Production Profiles Generated from Min, Mid and Max Case Fracture Models.

Table 1—k_{maxfx}/k_{minfx} Ratio Sensitivity Analysis.

Scenario	Impact	
	Plateau Length	Pulse Test
Average ratio of Mid, with Min and Max cutoff	Extend by 6 months	0.06 psi/week
Ratio of Min in all grid cells	Extend by 6 months	0.06 psi/week
Ratio of Max in all grid cells	Extend by 13 months	0.06 psi/week

Forward Plan

With the pressure decline from the field production, the reservoir behavior may change with time and this can help understand more on the interaction between fracture and matrix. Therefore, with the reservoir surveillance program, reservoir pressure and field production should be monitored closely. Dual-porosity dual-permeability model may also be considered if the current pseudo-fracture model is deemed insufficient. Fracture data acquisition during future infill drilling will also help to characterize the fractures and evaluate their impact on reservoir performance. Production implications from offset fields of similar kind may also shed light on field development.

It should be kept in mind that reservoir modelling effort never stops. Rather, it is an ever-green process that dynamic reservoir performance information should be incorporated to update the model periodically or when seeing any gaps to improve its accuracy of prediction to assist optimal reservoir management.

Acknowledgment

The authors thank the management of UECSL and CNPC for their permission to publish this paper. Special thanks to fracture subject matter experts SMEs for their advices and support on fracture characterization and reservoir modelling and history match.

Conflicts of Interest

The author(s) declare that they have no conflicting interests.

References

Aguilera, R. 1980. *Naturally Fractured Reservoirs*. Tulsa, USA: Pennwell Publishing Company.

Angerer, E., Neff, P., and Abbasi, I. et al. 2011. Integrated Reservoir Characterization of a Fractured Basement Reservoir. *The Leading Edge* **30**(12):1408-1413.

Awdal, A., Healy, D., and Alsop, G. I. 2016. Fracture Patterns and Petrophysical Properties of Carbonates Undergoing Regional Folding: A Case Study from Kurdistan, N Iraq. *Marine and Petroleum Geology* **71**(8): 149-167.

Bourbiaux, B., Basquet, R., and Daniel, J. 2005. Fractured Reservoirs Modelling: A Review of the Challenges and Some Recent Solutions. *First Break* **23**(9):33-40.

Kuchuk, F., Biryukov, D., and Fitzpatrick, T. 2015. Fractured-Reservoir Modeling and Interpretation. *SPE Journal* **20**(5):78-96. SPE-176030-PA.

Bratton, T., Canh, D., and Que, N. 2006. The Nature of Naturally Fractured Reservoirs. *Oilfield Review* **18**(2): 4-23.

Crain, E. 2017. Crain's Petrophysical Handbook (online). https://www.spec2000.net/22-fracloc1.htm, accessed June 2017.

Fekete Associates Inc., Dual porosity.
http://www.fekete.com/SAN/TheoryAndEquations/WellTestTheoryEquations/Dual_Porosity.htm, accessed June 2017.

Galuppoc C., Toscani, G., Turrini, C., et al. 2016. Fracture Patterns Evolution in Sandbox Fault-Related Anticlines. *Italian Journal of Geosciences* **135**(1):5-16.

Kappa DDA Book v4.30.01. https://www.kappaeng.com/documents/flip/dda/, accessed June 2017.

Lee, J. and Wattenbarger, R.1996. *Gas Reservoir Engineering*. Textbook Series, SPE, Richardson, Texas.

Lyons, W.C and Plisga, G. J. 2004. *Standard Handbook of Petroleum & Natural Gas Engineering* (*Second Edition*). Oxford, UK: Gulf Professional Publishing.

Narr, W. 1996. Estimating Average Fracture Spacing in Subsurface Rock. *AAPG Bulletin* **80**(10): 1565–1586.

Narr, W., Schechter, D., and Thompson, L. 2006. *Naturally Fractured Reservoir Characterization*. Society of Petroleum Engineers, Richardson, Texas.

Narr, W., Fischer, D., Harris, M., et al. 2004. Understanding and Predicting Fractures at Tengiz–A Giant, Naturally Fractured Reservoir in The Caspian Basin of Kazakhstan. Search and Discovery Article #20057.

Nelson, R.A. 2001. *Geologic Analysis of Naturally Fractured Reservoirs (Second edition)*. Oxford, UK: Gulf Publishing.

Price, N. 1966. Fault and Joint Development in Brittle and Semi-Brittle Rock. *Pergamon Press* **32**(5):176-190.

Price, N. and Cosgrove, J. 1990. Analysis of Geological Structures. *Cambridge University Press* **128**(3)502-510.

Stearns, W. and Friedman, M. 1972. Reservoirs in fractured rock: Geologic Exploration Methods. In *Stratigraphic Oil and Gas Fields—Classification, Exploration Methods, and Case Histories* ed. Gould, H.R. Chap 16, 82–106.

Satter A. and Iqbal G. 2015. *Reservoir Engineering: The Fundamentals, Simulation, and Management of Conventional and Unconventional Recoveries*. Oxford, UK: Gulf Professional Publishing.

Minh Vo, SPE, is currently subsurface manager in Unocal East China Sea Ltd., where he has worked for the last 4+ years. He has had 25 years of experience in the oil and gas industry with multiple global locations. His research interests are in reservoir engineering, production optimization, and systems engineering. He holds several master's degrees from UNSW in petroleum engineering, from RMIT in systems engineering, and MBA from NYU.

San Su, AAPG, is a development geologist in Unocal East China Sea Ltd., where he has worked for 11 years. His research interests are in geology and geophysics, carbonate formation evaluation and characteristics. He holds bachelor's and master's degree in geoscience from China University of Geoscience, Beijing.

Jianjiang Lv, SPE, is production engineer in Unocal East China Sea Ltd., where he has worked for 7 years. His research interests are in production and reservoir engineering. He holds master's degree and Ph.D. from Southwest Petroleum University, both in petroleum engineering.

Chaohong Xiao, is a production engineer in Southwest Oil & Gas Field Company, where he has worked for 32 years. His research interests are in production engineering and daily field operations management. He holds BSc. degree from Southwest Petroleum University in petroleum engineering.